Fat suppression techniques (STIR vs. SPAIR) on diffusion-weighted imaging of breast lesions at 3.0 T: preliminary experience

Sofia Brandão · Luísa Nogueira · Eduarda Matos · Rita Gouveia Nunes · Hugo Alexandre Ferreira · Joana Loureiro · Isabel Ramos

S. Brandão (✉) · J. Loureiro · I. Ramos
Department of Radiology, Centro Hospitalar de São João-EPE/ Faculty of Medicine, University of Porto, Alameda Prof. Hernâni Monteiro, 4200-319 Porto, Portugal
e-mail: sofia.brand@gmail.com

J. Loureiro
e-mail: joanaploureiro@gmail.com

I. Ramos
e-mail: radiologia.hsj@mail.telepac.pt

L. Nogueira
Centro Hospitalar São João-EPE/Faculty of Medicine, University of Porto, Alameda Prof. Hernâni Monteiro, 4200-319 Porto, Portugal
e-mail: mlpnogueira@med.up.pt

L. Nogueira
School of Applied Health Sciences, Oporto Polytechnic Institute (ESTSP/IPP), Rua Valente Perfeito, 322, 4400-330 Vila Nova de Gaia, Portugal

E. Matos
Department of Health Community, Institute of Biomedical Sciences Abel Salazar of Porto University (ICBAS), Rua de Jorge Viterbo Ferreira, 228, 4050-313 Porto, Portugal
e-mail: ematos@icbas.up.pt

R. G. Nunes · H. A. Ferreira
Institute of Biophysics and Biomedical Engineering (IBEB), Faculty of Sciences, University of Lisbon, Campo Grande, 1749-016 Lisbon, Portugal
e-mail: rgnunes@fc.ul.pt

H. A. Ferreira
e-mail: hhferreira@fc.ul.pt

Abstract

Purpose The aim of this work was to perform a qualitative and quantitative comparison of the performance of two fat suppression techniques on breast diffusion-weighted imaging (DWI).

Materials and methods Fifty-one women underwent clinical breast magnetic resonance imaging, including DWI with short TI inversion recovery (STIR) and spectral attenuated inversion recovery (SPAIR). Four were excluded from the analysis due to image artefacts. Rating of fat suppression uniformity and lesion visibility were performed. Agreement between the two sequences was evaluated. Additionally, signal-to-noise ratio (SNR), contrast-to-noise ratio (CNR), and apparent diffusion coefficient (ADC) values for normal gland, benign and malignant lesions were compared. Receiver operating characteristic analysis was also performed.

Results From the 52 lesions found, 47 were detected by both sequences. DWI-STIR evidenced more homogeneous fat suppression ($p = 0.03$). Although these lesions were seen with both techniques, DWI-SPAIR evidenced higher score for lesion visibility in nine of them. SNR and CNR were comparable, except for SNR in benign lesions ($p < 0.01$), which was higher for DWI-SPAIR. Mean ADC values for lesions were similar. ADC for normal fibroglandular tissue was higher when using DWI-STIR ($p = 0.006$). Sensitivity, specificity, accuracy and area under the curve values were alike: 84.0 % for both; 77.3, 71.4 %; 80.9, 78.3 %; 82.5, 81.3 % for DWI-SPAIR and DWI-STIR, respectively.

Conclusion DWI-STIR showed superior fat suppression homogeneity. No differences were found for SNR and CNR, except for SNR in benign lesions. ADCs for lesions were comparable. Findings in this study are consistent with previous studies at 1.5 T, meaning that both fat suppression techniques are appropriate for breast DWI at 3.0 T.

Keywords Magnetic resonance imaging · Breast diffusion-weighted imaging · Fat suppression techniques · Image quality

Introduction

Research in breast magnetic resonance imaging (MRI) reports diffusion-weighted imaging (DWI) as a useful technique to improve lesion characterisation. To date, most of the published work relates to apparent diffusion coefficient (ADC) quantification at 1.5 T [1, 2], and publications focusing on 3.0 T are still scarce. The ADC value quantifies the signal intensity attenuation between at least two diffusion-weighted images with different *b* values [3]. The signal intensity decrease depends on both tissue characteristics and image parameters. Malignant breast lesions, usually display higher signal intensity when compared to normal tissue or benign lesions, reflecting more compact barriers to water motion [3]. Apart from tissue architecture, voxel signal intensity is also related to the pulse sequence parameters, e.g. echo time, matrix size, *b* value and the fat suppression technique.

Fat suppression is essential to eliminate the lipid signal and also to reduce image artefacts. If suppression is not homogeneous it may eventually impair lesion detection and ADC measurement [3]. Also, signal-to-noise ratio (SNR) and contrast-to-noise ratio (CNR) are strongly correlated with the quality of fat suppression. For that purpose, different techniques can be combined with breast DWI, each with their own advantages and drawbacks. Fat saturation (FatSat) methods are based on frequency-selective radiofrequency (RF) pulses that only excite fat spins. Chemical shift selective (CHESS) pulses are easily included in most pulse sequences but work poorly in regions with inhomogeneous B0 [4], which may lead to insufficient fat suppression, especially when compared to short TI inversion recovery (STIR) [5]. As STIR uses a spatially selective 180° RF pre-pulse with short inversion time to suppress lipid signal, it is a more robust approach to cope with B0 inhomogeneities and susceptibility changes [3–6]. Nevertheless, the fact that STIR leads to an inherent T1-weighting, suppressing signal from tissues with T1 similar to fat is a limiting factor to its use.

In the case of spectral pre-saturation with inversion recovery (SPIR) and spectrally attenuated inversion recovery (SPAIR), spectral pre-saturation pulses are added to the inversion recovery module [7]. For T1- or T2-weighted fat suppression, SPAIR uses adiabatic (frequency-varying) inversion pulses [8] to invert fat spins, and a spoiler to destroy any residual transverse magnetisation. This process reduces the effect of B1 inhomogeneities, which are frequent on high-field MRI, but increases RF absorption rate [9].

Given that signal intensity may depend on the fat suppression technique, different options for breast DWI should be considered in the clinical setting, since it may affect lesion identification and the demarcation of the region-of-interest (ROI) to calculate the ADC. This may have a true impact on lesion classification, as the ADC value is used to distinguish benign from malignant lesions [10, 11].

Therefore, the purpose of this study was to compare STIR and SPAIR for breast DWI at 3.0 T, through the evaluation of the homogeneity of fat suppression and lesion detection, SNR and CNR. The ADC values for normal tissue and lesions, and diagnostic performance were also compared.

Materials and methods

Patients

A prospective study was developed to analyse the use of DWI in breast MRI at 3.0 T. The focus was to evaluate lesion classification by investigating the influence of several parameters of DWI, namely the best set of *b* values, the fat suppression technique, and signal intensity fitting models.

This preliminary study was carried out between July 2009 and January 2010, and includes the first sets of data. In that period, 51 women underwent clinical breast MRI with two different DWI pulse sequences. The Institutional Ethics Committee approved this work (protocol: CES 276/13), and all the patients gave their written informed consent.

Reasons for breast MRI included: screening of women with BRCA1 and 2 ($n = 5$), evaluation of suspicious lesions on ultrasound/mammography ($n = 27$); and pre-surgical staging ($n = 19$).

Acquisitions for premenopausal patients were done between the 7th and the 14th day of their menstrual cycles to exclude effects of hormonal fluctuations on ADC [3, 12]. Exclusion criteria included technical problems, patient noncooperation and motion artefacts. Histological results were the reference standards for lesion diagnosis.

MRI acquisition

The MR examinations were performed using a 3.0 T system (MAGNETOM Tim Trio, Siemens Medical Solutions,

Table 1 Scanning protocol for the DWI pulse sequences

Parameters	DWI	
Sequence	SS-SE-EPI	SS-SE-EPI
Fat suppression	STIR	SPAIR
Orientation	Sagittal	Sagittal
TR/TE (ms)	4,900/108	4,900/106
TI (ms)	240	–
FOV (mm^2)	250 × 250	250 × 250
Matrix	84 × 128	84 × 128
Slice thickness (mm)	5	5
Voxel size (mm^3)	3 × 2×5	3 × 2×5
Number of slices	16	16
NEX	3	3
Bandwidth (Hz/pixel)	1,628	1,628
Scan time (min)	5:58	5:58
b values (s/mm^2)	50, 200, 400, 600, 800, 1,000, 2,000, 3,000	50, 200, 400, 600, 800, 1,000, 2,000, 3,000

DWI diffusion-weighted imaging, *FOV* field-of-view, *NEX* number of excitations, *SS-SE-EPI* single shot-spin echo-echoplanar imaging, *TR/TE* repetition time/echo time, *TI* inversion time

Erlangen, Germany) equipped with a dedicated four-channel breast phased-array RF coil.

The MRI protocol included 5-mm-thick axial T2w-FSE and sagittal STIR-FSE and DWI images, followed by a 0.9-mm-thick dynamic contrast-enhanced axial images, and 1-mm-thick sagittal T1w-GRE water excitation post-contrast images. Single-shot-SE-EPI-STIR and -SPAIR pulse sequences with multiple *b* values were acquired unilaterally in the sagittal plane for both breasts before gadolinium injection. Parallel imaging (acceleration factor of two), a saturation slab covering the thorax, and volume shimming were used [13]. Table 1 shows further details. Total examination time was approximately 38 min.

Image analysis

A senior radiologist, with 5 years experience on breast MRI (J.L.) prospectively reported the clinical MR examinations according to the BIRADS-MRI lexicon [14].

Conventional and DWI pulse sequences were transferred to a workstation. The dynamic contrast-enhanced acquisition was reconstructed a posteriori in the sagittal plane. To calculate the ADC value for this work, the monoexponential model was applied using the *b* values 50, 200, 400, 600, 800 and 1,000 s/mm^2.

Based on the lesion description in the clinical MR report, and using sagittal STIR-FSE and dynamic contrast-enhanced images to locate them, two readers (S.B. and L.N.) analysed the DWI datasets in consensus. Readers were blinded to the histopathological results.

Visual assessment

Image quality was assessed for both uniformity of fat suppression and lesion visibility. Uniformity of fat suppression was encoded as follows: 0—homogeneous fat suppression; 1—evidence of heterogeneous fat suppression, though with no impairment in lesion analysis; 2—images with major fat suppression problems that make lesion identification unfeasible. Lesion visibility was scored by using: 0—lesion is not seen; 1—lesion is poorly seen, requiring T1-w post-contrast images for identification; 2—lesion is visible, but not as conspicuous as in T1-w post-contrast images; 3—the lesion is easily visible, equivalent to T1-w post-contrast images. These variables were dichotomised for further statistical analysis. For uniformity of fat suppression, the score of 0 was opposed to scores 1 and 2 that were grouped (given that for either, fat suppression was not homogeneous). Regarding lesion visibility, scores of 0 were given to "non-visible" lesions, while scores 1, 2 and 3 were considered as "visible". The distribution of visible lesions by score was recorded. Additionally, the strength of agreement between STIR and SPAIR was assessed for the two variables.

Quantitative assessment

Using the STIR and dynamic contrast-enhanced images for visual guidance, fixed circular 0.25 cm^2 regions-of-interest (ROIs) were manually drawn on the b400 s/mm^2 diffusion images, and then copied on to the other *b* values and the ADC map. The ROIs were drawn in the lesions so as to only include the area with highest signal intensity. For

Table 2 Main features of the lesions in the sample

Characteristics	Mean ± SD or *N*
No. of lesions on DCE	52
No. of lesions on DWI-STIR	47
No. of lesions on DWI-SPAIR	47
No. of malignant lesions	25
Size of malignant lesions (mm)	23 ± 13
Malignant histopathological subtype	
Ductal carcinoma in situ (DCIS)	4
Lobular carcinoma in situ (LCIS)	1
Invasive ductal carcinoma (IDC)	11
Invasive lobular carcinoma (ILC)	7
Mucinous carcinoma	1
Other malignant (NOS)[a]	1
No. of benign lesions	22
Size of benign lesions (mm)	13 ± 5
Benign histopathological subtype	
Fibroadenoma	9
Epithelial proliferative lesion	4
Papilloma	1
Complex sclerosing lesion	4
Fibrocystic changes	2
Complex cystic lesion	2

DCE dynamic contrast enhancement, *DWI-SPAIR* diffusion-weighted imaging-spectrally attenuated inversion recovery, *DWI-STIR* diffusion-weighted imaging-short tau inversion recovery, *N* absolute number, *SD* standard deviation

[a] Other malignant lesions (NOS—not otherwise specified)

fibroglandular tissue demarcation, the ROI was positioned in the mid-sagittal slice, behind the nipple and avoiding fat. The selection of the b400 s/mm^2 images was based on a compromise of having image contrast between the lesion core and its outer limits, but still higher SNR than that of b1,000 s/mm^2.

SNR and CNR for each type of lesion and normal fibroglandular tissue (measured on the contralateral breast) were calculated at b1,000 s/mm^2 using the appropriate equations [15, 16]. According to Rahbar et al. [17], the CNR was considered to be positive when the lesion's signal intensity was higher than normal background breast tissue.

Mean values of signal intensity, SNR, CNR and ADC were compared between DWI-ST IR and DWI-SPAIR for benign and malignant lesions, and normal fibroglandular tissue. The ADC cutoff values for each fat suppression technique were estimated. Diagnostic performance of the ADC values was also calculated for each fat suppression technique.

Statistical analysis

IBM SPSS 20.0 software was used to perform the statistical analysis. A descriptive analysis was used to characterise our sample. The McNemar test was adopted to evaluate the homogeneity of fat suppression and lesion visibility. For the two qualitative variables, the strength of agreement between STIR and SPAIR was assessed using the Kappa coefficient (k), classified as poor (<0.2); fair (0.21–0.4); moderate (0.41–0.6), good (0.61–0.8) and very good (0.81–1.0) [18]. The Wilcoxon rank test was used to compare the mean values of signal intensity, SNR, CNR and ADC for each of the fat suppression techniques and tissues (normal fibroglandular tissue, benign and malignant lesions). The differences in the ADC values between benign and malignant lesions for each fat suppression technique were assessed by the Mann–Whitney test.

The ADC optimal cutoff point was selected based on the receiver operating characteristic (ROC) curve. Sensitivity, specificity and accuracy were calculated for both fat suppression techniques. The area under the curve (AUC) was compared. Statistical significance was considered for $p < 0.05$.

Results

Subjects and lesions

From the 51 patients initially enrolled in this study, four were excluded due to the presence of motion artefacts on the DWI, which prevented image analysis. From the remaining 47 women, 38 were menopausal (mean age 45.5 ± 2.1 years, range 30–64 years).

From the 52 lesions detected with the dynamic contrast-enhanced pulse sequence, 47 were characterised by DWI-STIR and DWI-SPAIR. Lesions smaller than 7.0 mm were not seen on the DW images, corresponding to two lobular carcinoma in situ with 6.0 mm, one epithelial proliferative lesion with 6.5 mm and two fibrocystic changes. Mean size was of 18.0 ± 11.0 mm, although malignant lesions were larger than benign ones (23 ± 13 mm vs. 13 ± 5 mm).

Histological confirmation was obtained for all mentioned lesions following this study. Table 2 shows the lesion characteristics. Out of the 47 lesions identified in the DWI sequence, 25 were malignant tumours from which 11 were ductal carcinoma and seven were invasive lobular carcinoma. The most frequent of the 22 benign lesions was the fibroadenoma ($n = 9$).

Qualitative assessment

The percentage of images with homogeneous fat suppression was higher for DWI-STIR than for DWI-SPAIR, 85.1 % (40/47) versus 72.3 % (34/47) ($p = 0.03$). There was good accord between the two techniques, $k = 0.64$ (95 % CI 0.36–0.88).

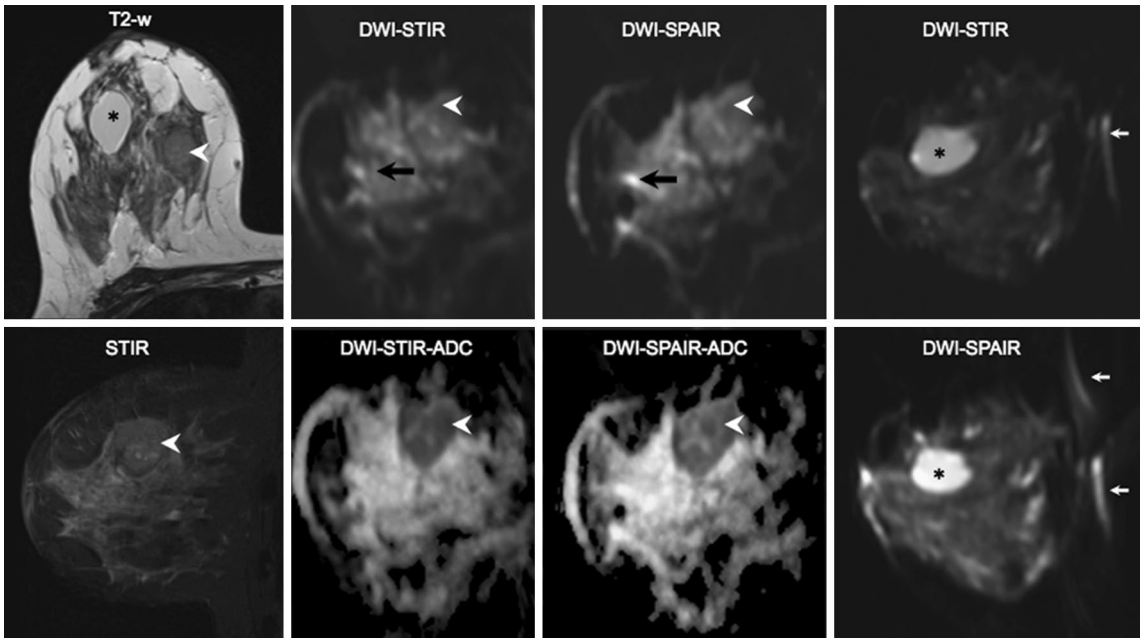

Fig. 1 Thirty-eight-year-old woman with an invasive ductal carcinoma (IDC) and a large cyst in the right breast. Morphological (*left column*) and DWI-STIR (diffusion-weighted imaging-short tau inversion recovery) and -SPAIR (spectrally attenuated inversion recovery) images (b50 s/mm^2) and the corresponding apparent diffusion coefficient (ADC) maps show a large tumour in the upper quadrant (*arrowhead*) with diffusion restriction and low ADC. Susceptibility artefacts in the interface between the adipose and the fibroglandular tissues (*black arrows*), as well as in the anterior thoracic wall (*white arrows*) are far more evident on the DWI-SPAIR images

All the lesions detected on DWI were visible on both sequences. Nine lesions were rated with score 3 in DWI-SPAIR, and classified with score 2 in DWI-STIR. For 29 lesions (61.7 %) the same score was achieved by both techniques. A moderate agreement was found, with $k = 0.43$ (95 % CI 0.21–0.64).

Figure 1 illustrates the use of the two fat suppression techniques in the case of a 38-year-old woman with an invasive ductal carcinoma on the right breast (superior quadrant), near a large simple cyst.

Quantitative analysis

The signal intensity decreased with the increasing *b* values. Mean values were higher in the DWI-SPAIR for all *b* values ($p = 0.001$), and for both lesions and normal breast. At b1,000 s/mm^2, which is the most frequently used diffusion-weighting factor, *p* values were $p = 0.04$, $p = 0.001$, and $p = 0.02$ for fibroglandular tissue, benign and malignant lesions, respectively. Malignant tumours presented the highest signal intensity as opposed to the normal fibroglandular gland. Table 3 displays results of the quantitative analysis of the data. DWI-SPAIR only evidenced higher SNR for benign lesions ($p < 0.01$). Both DWI sequences showed similar CNR for benign and malignant lesions. There were no differences between ADC values except for the normal fibroglandular tissue ($p < 0.01$). The AUC was similar for DWI-STIR and -SPAIR ($p = 0.78$). Both techniques showed sensitivity of 84.0 %, but DWI-SPAIR evidenced slightly higher specificity and accuracy.

The larger AUC was obtained for the cutoff ADC values of 1.54 and 1.49 ($\times 10^{-3}$ mm^2/s), respectively, for DWI-SPAIR and DWI-STIR. Two more false positives were found for DWI-STIR (two fibroadenomas, two fibrocystic changes, one epithelial proliferative lesion, one sclerosing lesion), than for DWI-SPAIR (two fibroadenomas, one fibrocystic change and one epithelial proliferative lesion). Both techniques detected four false-negative cases: one mucinous carcinoma, and three invasive ductal carcinoma for DWI-SPAIR; and one mucinous carcinoma, one ductal carcinoma in situ, and two invasive ductal carcinoma for DWI-STIR.

Discussion

Papers regarding breast DWI at 3.0 T are still scarce, but this field strength seems to be advantageous for characterising breast lesions [19–22]. Image quality is very important, as lesion characterisation and ADC quantification directly depend on the ability to locate it and measure its signal intensity.

As DWI is mostly based on echoplanar imaging, it is quite challenging at high field because B0- and B1

Table 3 Comparison of signal-to-noise ratio, contrast-to-noise ratio and apparent diffusion coefficient at b1,000 s/mm^2, in normal fibroglandular tissue, benign and malignant lesions, and diagnostic performance of diffusion-weighted imaging (DWI)-spectrally attenuated inversion recovery and DWI-short-tau inversion recovery

	DWI-SPAIR	DWI-STIR	*p* value
$SNR_{normal\ gland}$	15.8 ± 0.6	10.62 ± 0.6	0.16
$SNR_{benign\ lesions}$	17.3 ± 0.8	11.17 ± 0.5	<0.01*
$CNR_{benign\ lesions}$	1.1 ± 0.1	1.09 ± 0.08	0.12
$SNR_{malignant\ lesions}$	18.3 ± 0.3	16.84 ± 0.2	0.68
$CNR_{malignant\ lesions}$	1.2 ± 0.1	1.17 ± 0.2	0.08
$ADC_{normal\ gland}$ ($\times 10^{-3}$ mm^2/s)	1.79 ± 0.29	1.88 ± 0.39	<0.01*
$ADC_{benign\ lesions}$ ($\times 10^{-3}$ mm^2/s)	1.68 ± 0.39	1.72 ± 0.47	0.40
$ADC_{malignant\ lesions}$ ($\times 10^{-3}$ mm^2/s)	1.19 ± 0.36	1.21 ± 0.437	0.35
Cutoff ($\times 10^{-3}$ mm^2/s)	1.54	1.49	–
Sensitivity	84.0 %	84.0 %	–
Specificity	77.3 %	71.4 %	–
Accuracy	80.9 %	78.3 %	–
AUC	82.5 % (68.7–92.1 %)	81.3 % (67.1–91.3 %)	0.78

ADC apparent diffusion coefficient, *SNR* signal-to-noise ratio, *CNR* contrast-to-noise ratio, *DWI-SPAIR* diffusion-weighted imaging-spectrally attenuated inversion recovery, *DWI-STIR* diffusion-weighted imaging-short tau inversion recovery, *AUC* area under the curve

* Statistically significant

inhomogeneity-related artefacts are considerably amplified. They lead to areas of signal intensity dropout, image blurring and ghosting, geometric distortion and chemical shift artefacts. Therefore, the fat suppression technique should be as robust as possible. As FatSat methods are more prone to artefacts [4, 6], water excitation, Dixon, STIR or SPAIR techniques may be preferred at 3.0 T. Also, recent scanners can apply dual-source RF excitation with independent RF shimming that improves signal homogeneity and fat suppression by reducing the dielectric effects, thus enabling the use of short TRs and low RF absorption rate (SAR) [23, 24].

In our study, there were no major fat suppression problems in the DWI datasets that prevented lesion identification. To maximise scanning success rate, we have established some strategies to improve image quality, such as the use of volume shimming, manual lipid frequency peak identification, small field-of-view and the use of parallel imaging [2]. Despite potentially resulting in a slight decrease in SNR, parallel imaging shortens acquisition time [25] with no major impact on ADC values [2]. DWI-STIR outperformed DWI-SPAIR in fat suppression homogeneity in six cases, which was most probably related to its higher insensitivity to B0 inhomogeneities and susceptibility artefacts [3–6].

Ninety percent of the lesions were detected in both sequences, in accordance to what was found by other authors [1, 26]. The fact that nine lesions were more easily visible on the DWI-SPAIR when compared to DWI-STIR is perhaps related to its higher SNR and CNR. Matsuoka et al. [19] found high visibility scores at 3.0 T even for lesions smaller than 10 mm. The minimum lesion size on DWI in this study, as defined by the longest dimension on the dynamic acquisition, was 7.4 mm, which is acceptable considering the 5-mm slice thickness. A decrease in the slice thickness to 3–4 mm could have enabled the detection of even those small lesions, although at the cost of lowering the SNR.

Normal fibroglandular tissue presented lower signal intensity when compared to lesions at b1,000 s/mm^2, due to a less compact structure and good suppression of the fat component. We found higher signal intensity, SNR and CNR values on DWI-SPAIR when compared to DWI-STIR, although not all statistically different, an exception being the SNR for benign lesions. Even though these results could perhaps be related to the variety of their histological types, this can potentially be explained by the fat suppression technique itself [27, 28], as all other geometric and timing parameters were kept the same. Although these results require additional confirmation, it is known that SPAIR enhances the lesion-to-background contrast [29]. On the contrary, the STIR technique saturates other tissues with very similar T1 values analogous to that of fat. Moreover, most tissues recover more slowly than fat and, therefore, the SNR decreases.

As in other studies, malignant lesions presented higher SNR and CNR at 1,000 mm^2/s when compared to benign ones in both sequences, due to their increased cellular components and diffusion restriction. Previous work from Bogner et al. [16] and Takanaga et al. [30] at 3.0 T found a

higher CNR for malignant lesions at b850 and b500 s/mm^2, respectively. The histological type of the lesions or the fat suppression technique may explain these differences, as the authors used DWI-STIR and DWI-SPECIAL (spectral inversion at lipid) (similar to SPIR) pulse sequences, respectively.

The ADC value is used to differentiate between benign and malignant breast lesions. The differences in the scanners' hardware, magnetic field strength and imaging protocol must be taken into account when comparing different studies. Previous studies from Matsuoka et al. [19] and Lo et al. [31] at 3.0 T reported ADC values for malignant lesions of 0.98 ± 0.16 and 1.01 ± 0.25 × 10^{-3} mm^2/s, while mean ADC for benign lesions was 1.47 ± 0.30 × 10^{-3} mm^2/s [31]. Our results are in agreement with these studies, with lower ADC for malignant lesions when compared to benign ones or normal fibroglandular tissue.

For quantitative ADC analysis, b1,000 s/mm^2 is usually applied [32, 33] as it is considered to be optimal for breast tumour imaging, because it enables good suppression of normal mammary gland and higher signal intensity from lesions [25]. In a meta-analysis published by Chen et al. [34] for the subgroup of studies using *b* values of 1,000 s/mm^2, the ranges of minimum and maximum ADC values for malignant and benign lesions were 0.91–1.21 and 1.39–1.61 (×10^{-3} mm^2/s), respectively. Our results are similar to the literature, although the mean ADC for the benign lesions in our sample is slightly higher than these, probably reflecting some degree of heterogeneity in their subtypes. The ADC values for the two fat suppression techniques were very similar except for the normal gland ($p < 0.01$). In our opinion, one should be careful when interpreting these preliminary results, as the sample size is small. Nevertheless, the most probable explanation is that spectral-selective methods such as SPAIR only suppress the ~3.4 ppm lipid signals, without affecting minor lipid peaks near the water resonance, whereas STIR suppresses all tissues that have short T1 and low-ADC fat constituents, thus increasing the ADC.

The cutoff values showing the higher AUC were 1.54 and 1.49 (×10^{-3} mm^2/s), respectively, for DWI-SPAIR and DWI-STIR. Sensitivity was 84.0 % for both fat suppression techniques; with specificity and accuracy rates of 77.3 and 71.4 %, and 80.9 and 78.3 %, respectively, which is slightly lower than other authors have reported [31, 32, 35, 36]. This may be related to the differences in the DWI pulse sequence parameters.

Both cutoff points resulted in a low number of false-negative and false-positive cases. Two more false positives were found for DWI-STIR (two fibroadenomas, two fibrocystic changes, one epithelial proliferative lesion, one sclerosing lesion) than for DWI-SPAIR (two fibroadenomas, one fibrocystic change and one epithelial proliferative lesion). The increased cellularity in some benign lesions was the probable cause for the false-positive cases. The additional complex sclerosing lesion found when the DWI-STIR cutoff point was 1.49 × 10^{-3} mm^2/s may be associated to the presence of different fibrotic degree and proliferative cell activity that constrain water diffusion and decrease the ADC value [37–40] that, in our study, was similar to malignant lesions.

Concerning the false negatives, both techniques showed four misclassified lesions, three of which were misleading lesions in the same patients (one mucinous carcinoma and two invasive ductal carcinomas). The high ADC of mucinous carcinoma may be due to the presence of mucus in the extracellular space and the decreased cellularity [3, 37], whereas invasive ductal carcinomas are often heterogeneous and have haemorrhagic focus. The false negative on DWI-STIR was a low-grade ductal carcinoma in situ, which may have ambiguous signal intensity, even at higher *b* values, due to rapid signal decay [10, 26, 41].

There are certain limitations in our study. First, the small sample size will require future work to confirm these preliminary results. Second, the scanning time for the clinical protocol and both the DWI-STIR and -SPAIR sequences was almost 40 min, resulting in a few cases of motion artefacts. However, an optimised acquisition with only two *b* values (b50 and 1,000 s/mm^2) would enable reducing the TE and shorten the acquisition time. Although performing two unilateral acquisitions may increase the scanning time, the use of small field-of-view for sagittal imaging enables good spatial resolution, better volume shimming and less magnetic susceptibility phenomena.

To further complement our results, a comparative analysis of nonparallel imaging will be performed, to check its benefit on image quality. Additionally, it would also be desirable to test the performance of the slice-selection gradient reversal method for fat suppression [42]. This method seems promising, achieving homogenous fat suppression with reduced acquisition time and SAR, which is particularly beneficial at high field strength.

Even though STIR enabled more homogeneous fat suppression, SPAIR provided better visibility for some lesions. The SNR and CNR were higher for DWI-SPAIR, although not statistically significant except for benign lesions. ADC values for malignant and benign lesions were similar. Specificity and accuracy were slightly higher for DWI-SPAIR. If the DW images were to be used on their own, more than 81 % of the lesions would be correctly diagnosed. In conclusion, STIR- and SPAIR-based DW images were suited to identify and characterise breast lesions at 3.0 T. Future work will include a higher number of lesions to confirm these preliminary results.

References

1. Belli P, Costantini M, Bufi E et al (2010) Diffusion-weighted imaging in breast lesion evaluation. Radiol Med 115:51–69
2. Jin G, An N, Jacobs MA, Li K (2010) The role of parallel diffusion-weighted imaging and apparent diffusion coefficient (ADC) map values for evaluating breast lesions: preliminary results. Acad Radiol 17:456–463
3. Woodhams R, Ramadan S, Stanwell P et al (2011) Diffusion-weighted imaging of the breast: principles and clinical applications. Radiographics 31:1059–1084
4. Takahara T, Imai Y, Yamashita T et al (2004) Diffusion weighted whole body imaging with background body signal suppression (DWIBS): technical improvement using free breathing, STIR and high resolution 3D display. Radiat Med 22:275–382
5. Kazama T, Nasu K, Kuroki Y et al (2009) Comparison of diffusion-weighted images using short inversion time inversion recovery or chemical shift selective pulse as fat suppression in patients with breast cancer. Jpn J Radiol 27:163–167
6. Bitar R, Leung G, Perng R et al (2006) MR pulse sequences: what every radiologist wants to know but is afraid to ask. Radiographics 26:513–537
7. Ribeiro MM, Rumor L, Oliveira M et al (2013) STIR, SPIR and SPAIR techniques in magnetic resonance of the breast: a comparative study. JBiSE 6:395–402
8. Tannús A, Garwood M (1997) Adiabatic pulses. NMR Biomed 10:423–434
9. Luna A, Ribes R, Soto JA (2012) Diffusion MRI outside the brain: a case-based review and clinical applications. Springer-Verlag, Berlin, New York
10. Woodhams R, Matsunaga K, Kan S et al (2005) ADC mapping of benign and malignant breast tumors. Magn Reson Med Sci 4:35–42
11. Guo Y, Cai YQ, Cai ZL et al (2002) Differentiation of clinically benign and malignant breast lesions using diffusion-weighted imaging. J Magn Reson Imaging 16:172–178
12. Partridge SC, McKinnon GC, Henry RG, Hylton NM (2001) Menstrual cycle variation of apparent diffusion coefficients measured in the normal breast using MRI. J Magn Reson Imaging 14:433–438
13. Lee J, Lustig M, Kim DH, Pauly JM (2009) Improved shim method based on the minimization of the maximum off-resonance frequency for balanced steady-state free precession (bSSFP). Magn Reson Med 61:1500–1506
14. Agrawal G, Su MY, Nalcioglu O et al (2009) Significance of breast lesion descriptors in the ACR BI-RADS MRI lexicon. Cancer 115:1363–1380
15. Heverhagen JT (2007) Noise measurement and estimation in MR imaging experiments. Radiology 245(3):638–639
16. Bogner W, Gruber S, Pinker K et al (2009) Diffusion-weighted MR for differentiation of breast lesions at 3.0 T: how does selection of diffusion protocols affect diagnosis? Radiology 253:341–351
17. Rahbar H, Partridge SC, Eby PR et al (2011) Characterization of ductal carcinoma in situ on diffusion weighted breast MRI. Eur Radiol 21:2011–2019
18. Altman DG (1991) Practical statistics for medical research. Chapman & Hall, London
19. Matsuoka A, Minato M, Harada M et al (2008) Comparison of 3.0-and 1.5-tesla diffusion-weighted imaging in the visibility of breast cancer. Radiat Med 26:15–20
20. Lourenço AP, Donegan L, Kahil H, Mainiero MB (2014) Improving outcomes of screening breast MRI with practice evolution: initial clinical experience with 3T compared to 1.5T. J Magn Reson Imaging 39:535–539
21. Rahbar H, Partridge SC, DeMartini WB et al (2013) Clinical and technical considerations for high quality breast MRI at 3 Tesla. J Magn Reson Imaging 37:778–790
22. Butler RS, Chen C, Vashi R et al (2013) 3.0 Tesla vs 1.5 Tesla breast magnetic resonance imaging in newly diagnosed breast cancer patients. World J Radiol 5:285–294
23. Mürtz P, Kaschner M, Träber F et al (2012) Evaluation of dual-source parallel RF excitation for diffusion-weighted whole-body MR imaging with background body signal suppression at 3.0 T. Eur J Radiol 81:3614–3623
24. Rahbar H, Partridge SC, DeMartini WB et al (2012) Improved B1 homogeneity of 3 Tesla breast MRI using dual-source parallel radiofrequency excitation. J Magn Reson Imaging 35:1222–1226
25. Kuroki Y, Nasu K (2008) Advances in breast MRI: diffusion-weighted imaging of the breast. Breast Cancer 15:212–217
26. Kuroki S, Kuroki Y, Nasu K et al (2007) Detecting breast cancer with non-contrast MR imaging: combining diffusion-weighted and STIR imaging. Magn Reson Med Sci 6:21–27
27. Thomassin-Naggara I, De Bazelaire C, Chopier J et al (2013) Diffusion-weighted MR imaging of the breast: advantages and pitfalls. Eur J Radiol 82:435–443
28. Partridge SC, Singer L, Sun R et al (2011) Diffusion-weighted MRI: influence of intravoxel fat signal and breast density on breast tumor conspicuity and apparent diffusion coefficient measurements. Magn Reson Imaging 29:1215–1221
29. Udayasankar UK, Martin D, Lauenstein T et al (2008) Role of spectral presaturation attenuated inversion-recovery fat-suppressed T2-weighted MR imaging in active inflammatory bowel disease. J Magn Reson Imaging 28:1133–1140
30. Takanaga M, Hayashi N, Miyati T et al (2012) Influence of b-value on the measurement of contrast and apparent diffusion coefficient in 3.0 Tesla breast magnetic resonance imaging. Nihon Hoshasen Gijutsu Gakkai Zasshi 68:201–208
31. Lo GG, Ai V, Chan JK, Li KW et al (2009) Diffusion-weighted magnetic resonance imaging of breast lesions: first experiences at 3 T. J Comput Assist Tomogr 33:63–69
32. Sonmez G, Cuce F, Mutlu H et al (2011) Value of diffusion-weighted MRI in the differentiation of benign and malign breast lesions. Wien Klin Wochenschr 123:655–661
33. Tsushima Y, Takahashi-Taketomi A, Endo K (2009) Magnetic resonance (MR) differential diagnosis of breast tumors using apparent diffusion coefficient (ADC) on 1.5-T. J Magn Reson Imaging 30:249–255
34. Chen X, Li WL, Zhang YL et al (2010) Meta-analysis of quantitative diffusion-weighted MR imaging in the differential diagnosis of breast lesions. BMC Cancer 10:693
35. Inoue K, Kozawa E, Mizukoshi W et al (2011) Usefulness of diffusion-weighted imaging of breast tumors: quantitative and visual assessment. Jpn J Radiol 29:429–436
36. Palle L, Reddy B (2009) Role of diffusion MRI in characterizing benign and malignant breast lesions. Indian J Radiol Imaging 19:287–290
37. Woodhams R, Kakita S, Hata H et al (2009) Diffusion-weighted imaging of mucinous carcinoma of the breast: evaluation of apparent diffusion coefficient and signal intensity in correlation with histologic findings. AJR Am J Roentgenol 193:260–266
38. Pereira FP, Martins G, Carvalhaes de Oliveira RV (2011) Diffusion magnetic resonance imaging of the breast. Magn Reson Imaging Clin N Am 19:95–110

39. Baltzer PAT, Dietzal M, Vag T (2009) Diffusion weighted imaging—useful in all kinds of lesions? A systematic review. Eur Radiol 19:S765–S769
40. Hatakenaka M, Soeda H, Yabuuchi H et al (2008) Apparent diffusion coefficients of breast tumors: clinical application. Magn Reson Med Sci 7:23–29
41. Iima M, Le Bihan D, Okumura R et al (2011) Apparent diffusion coefficient as an MR imaging biomarker of low-risk ductal carcinoma in situ: a pilot study. Radiology 260:364–372
42. Nagy Z, Weiskopf N (2008) Efficient fat suppression by slice-selection gradient reversal in twice-refocused diffusion encoding. Magn Reson Med 60:1256–1260